

Plasma deposition and properties of composite metal/polymer and metal/hard carbon films

H. Biederman, L. Martinů, D. Slavínská and I. Chudáček

Department of Polymer Physics, Faculty of Mathematics and Physics, Charles University, V Holešovičkách 2, 180 00 Praha 8, Czechoslovakia

Abstract - The growing interest in novel materials has promoted the investigation of two-component composite materials formed by small metal inclusions incorporated in an organic insulating medium. In this paper the recent knowledge of composite thin films composed of metal grains dispersed in the matrix of a plasma deposited polymer or a hard carbon is reviewed. The most important deposition techniques are presented and the relation between the deposition processes, the film microstructure and resulting film properties (especially optical and electrical) are discussed. The film characteristics are illustrated by the latest results from our laboratory.

INTRODUCTION

Over the past decade there has been a growing interest in the study of composite thin films because of the prospect to fabricate coatings with novel properties. At the beginning the main interest was in the systems composed of a metal and a metal oxide (or inorganic dielectric) which are sometimes called cermet (ref.1). However, in recent years growing attention has been paid to the composite systems which use as the dielectric phase an organic material - plasma polymer or hard carbon (refs. 2-4). Polymer films can be prepared by vacuum evaporation (ref.5), but sputtering and mainly plasma polymerization were applied in more cases (refs. 2-5). Generally, the passage of a glow discharge in an organic gas or a vapour results in the deposition of a polymer coating on exposed surfaces. Researchers usually tried to avoid contamination from the metal electrodes or other reactor components until they realized that the incorporation of metals into the matrix of a plasma polymer may lead to a new class of thin film materials (ref.6). Some of them became aware of the effect of energetic particle bombardment and UV light irradiation on the growth, structure and properties of resulting deposits. Obtained coating character changed from polymer, to hard polymer and, finally, to a - C:H or DLC (diamond-like) as the energy of bombarding positive ions was raised in the case of an r.f. glow discharge excited in a hydrocarbon gas or vapour (ref.7). In several very recent studies a metal has been supplied by thermal evaporation into the growing a - C:H film suggesting an improvement of properties of these metal/organic thin film systems (refs. 8-18).

In this review we discuss basic physical properties of the above mentioned metal/plasma polymer or metal/hard carbon composite films in connection with their deposition processes which use sputtering, sputter etching or thermal evaporation for a metal supply.

PLASMA DEPOSITION TECHNIQUES AND PROCESSES

Several methods using low temperature plasmas for the preparation of metal/plasma polymer or hard carbon have been developed: a) plasma polymerization of an organic gas or vapour and simultaneous co-sputtering or etching of a metal from the target electrode (refs.2,19,20), b) evaporation of a metal and plasma polymerization of an organic gas or vapour (refs.21,22), c) sputtering from a composite polymer/metal target (ref.23). For complexity, plasma polymerization of an organometallic compound (refs.24-25) and simple vacuum evaporation of both polymer and metal (ref.27) should be mentioned here.

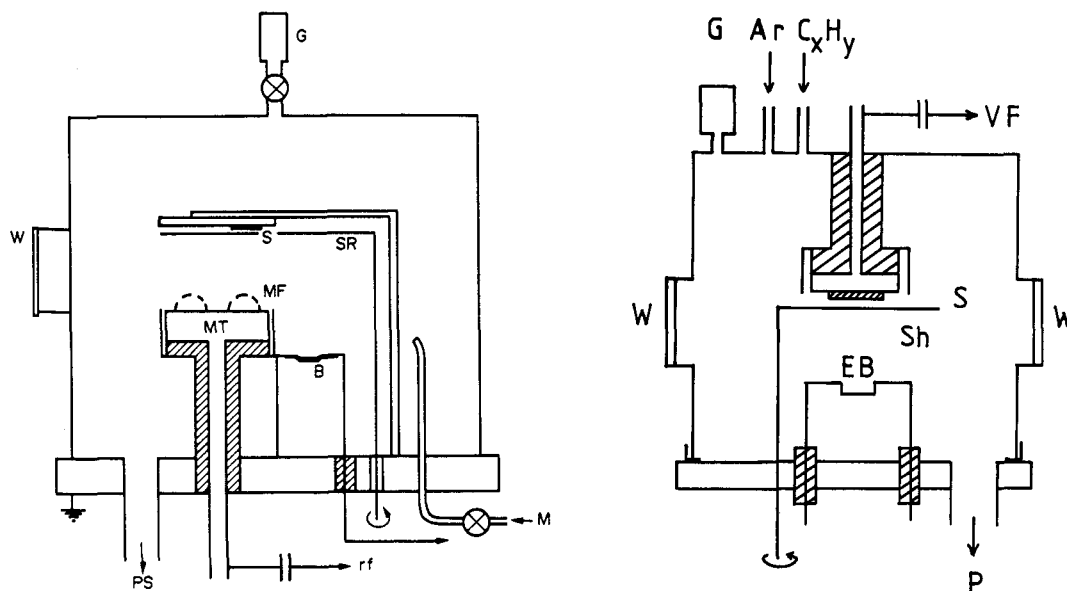


Fig. 1. - Schematic arrangement of the system for the deposition of:
 a) metal/plasma polymer films, b) metal/a-C:H films.
 MT-magnetron target, MF-tunnel magnetic field, S-substrate position,
 B(EB) - evaporation boat, P(PS)-pumping system, RF(VF)-to the power
 supply, M-monomer inlet, W-quartz window, G-vacuum gauge, SR(Sh)-
 shutter.

The first two methods presented above became most popular. The schematic deposition arrangement can be seen in Fig. 1a. It is a plan-parallel plate electrode system with the earthed substrate holder and insulated target electrode powered from an rf generator (13.56 MHz) with one terminal grounded. Capacitive coupling of this electrode by means of a blocking capacitor causes development of substantial dc negative self bias (U_B) and therefore sputtering or reactive ion etching (or both) of the target²⁸ providing thus a metal supply. The glow discharge which is excited by the mentioned target electrode in a monomer gas promotes plasma polymerization. Energetic electrons impact on monomer molecules in a gas phase and create a number of species. Free radicals are recognized of special importance as they are supposed to diffuse to the substrate where chain reactions, chains branching, terminations and crosslinking take place forming thus a solid polymeric component of the composite film (refs. 5, 29-31). If a planar magnetron is used as the excitation electrode (as shown in Fig. 1a) increased metal emission and plasma polymerization rates occur at the same power levels. Further increase of the metal emission may be achieved if we dilute a monomer using argon. In the discussed deposition arrangement (Fig. 1a) several halocarbon gases as CF_4 , C_2F_8 , C_2F_5Cl , C_2F_6 , etc. (refs. 2-4, 32, 33) have been successfully used. However, when hydrocarbon or organosilicon gases are applied a "poisoning" of the target by a solid deposit often takes place hampering metal emission (refs. 34, 35). In this case it is more convenient to supply a metal from an ordinary evaporation boat and the target electrode use only for the discharge excitation as it is sketched in Fig. 1b. It has been shown that both ways of metal emission lead to equivalent composite films (ref. 33).

Composite films grown on grounded or floating substrates are subjected to electron and ion bombardment and uv light irradiation. At usual discharge conditions floating or earthed substrate is negative against plasma potential (with the potential drop typically of the order of 10V). Positive ion bombardment with this average energy is of special importance as it enhances the plasma polymerization via production of surface free radicals (ref. 4). In the case of an ordinary planar magnetron mentioned the potential drop is lower and most of electrons are trapped by the tunnel magnetic field. The situation will change if we put an increased U_B on the substrate via capacitive coupling of an independent rf generator or by splitting the original rf power. The most straightforward is to place the substrate on the excitation electrode (see Fig. 1b) - an idea suggested in the case of hydrocarbon plasmas by L. Holland (ref. 7). When halocarbon gases are used

competitive reactive ion etching takes place simultaneously. We did not observe any deposit on silica or glass substrates with CF_4 gas and deposition turned into substrate etching when U_B exceeded - 100 V in the case of C_2F_3Cl (chlorotri fluoroethylene CTFE) (ref.36). E. Kay (ref.4) reported for C_2F_4 that solid carbonaceous deposit covered the metal target up to $U_B = -2600$ V. As it was mentioned above in the case of organosilicon or hydrocarbon gases a solid polymeric coating was always obtained. Increasing U_B in the latter case one moves from a polymer to a hard polymer and finally to a - C:H (DLC) film if U_B exceeds - 200 V. These films possess unusual properties - high electrical resistivity, hardness higher than sapphire, optical transparency in the infrared and chemical inertness. It has been suggested that a - C:H film is composed of DLC (tetrahedral), graphite like (trigonal) and polymeric components and voids. Considerable amount of hydrogen is trapped and bonded in the film (up to 25%) (refs.8, 38, 39). In order to reduce the amount of hydrogen we have used a mixture of CTFE with benzene at $U_B = -180$ V and observed that the deposition rate increased reaching peak U_B at 70%. However, hard a - C:H films changed into predominantly polymeric soft coatings (ref. 36,40). The same results obtained Sah (ref. 40) using fluorinated benzenes. Memming has shown recently by means of IR spectroscopy structural differences between hard polymer and a - C:H films (ref. 41). More details about a - C:H films may be found in the latest reviews (e.g.ref. 42, 43).

A metal can be simply incorporated into a growing a - C:H film by thermal evaporation (see Fig. 1b). In this way we have prepared composite metal/a - C:H films with metals as Au, Ag, Al and Cu (refs. 9-11, 36). Weissmantel et al (refs. 8, 12, 13) have used instead of usual rf diode system an ion plating system operating at 0.1 Pa in benzene and metals as Cr, Al and Ti were co - evaporated.

A dc post cathode cylindrical magnetron was used for reactive sputtering of stainless steel cathode in Ar/ C_2H_2 mixture (refs. 14-16) and this study was completed using planar magnetron.²The authors suggested that cathode was first covered with a - C:H which was subsequently sputtered off. The necessary bombardment of the layer growing on the substrate at a floating potential came from energetic neutrals reflected from the cathode. Nickel/carbon films were also prepared by dc reactive sputtering in an Ar/ CH_4 mixture in an diode system (ref. 17). Weissmantel et al. (ref. 13) have also reported metal/hard carbon films prepared by magnetron co-sputtering of graphite and Ti or Sn metals. Savvides and Window (ref. 44) announced "DLC films" prepared by magnetron sputtering of graphite using unbalanced planar magnetron. They claimed that the escaping beam of the discharge plasma (negative glow) caused negative biasing of the substrate and the growing deposit and attracted positive ion bombardment (up to 40 eV energy). Using such unbalanced planar magnetron in the geometrical set-up similar to that pictured in Fig. 1a metal hard/carbon films were deposited (ref. 18). Composite metal/graphite target was sputtered in Ar or Ar/propane mixture. Most of the attention has been paid to silver, but Au, Mo, Pt and Cu have also been examined.

As a great number of parameters influence the deposition procedure the deposition processes should be in situ monitored using a diagnostic technique. The optical emission spectroscopy is the simplest one. A convenient metal line is compared to a nearby positioned argon line or the intensity of the emission band of a typical radical. An example may be gold line at $\lambda = 267$ nm compared to the height of the band head belonging to the CF_2 radical at $\lambda = 265$ nm in the case of gold/plasma polymerized (pp) fluorocarbon films (ref. 45). More optical techniques are available e.g. actinometry etc. Mass spectroscopic techniques are very useful, e.g. quadrupole mass spectrometer as it was applied by E. Kay and his co-workers (ref. 4). Electric probe measurements are also very helpful in laboratory experiments (ref. 46) but difficult to be placed permanently into the production apparatus.

COMPOSITE FILM STRUCTURE

Metal/plasma polymer films

The composite film structure develops as a result of competitive processes of polymer formation and metal nucleation on the substrate surface. In principle, it depends on the individual deposition rates of both constituents but in fact the problem is very complex and many effects play an important role: sticking probability for individual species, surface migration in dependence on the actual surface temperature and specie energy, chemical reactivity, internal stresses etc.

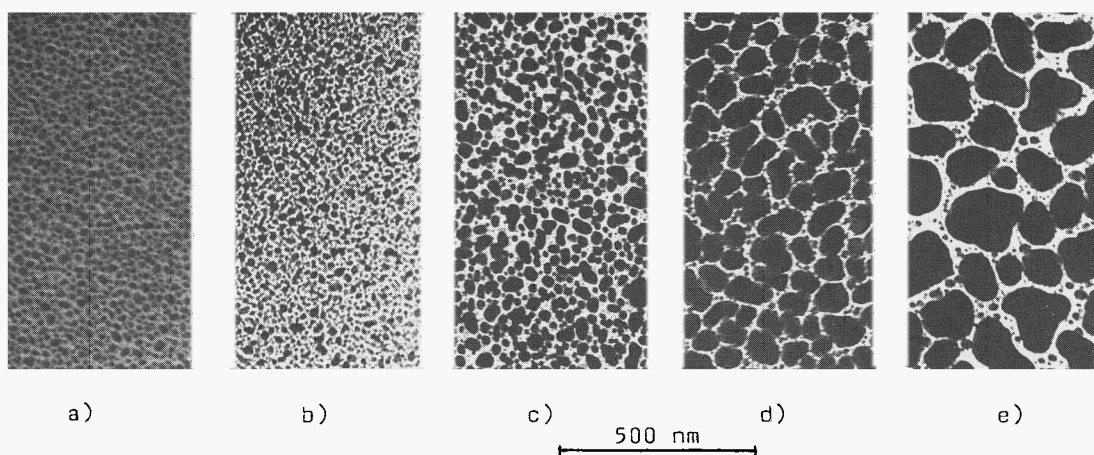


Fig. 2. Transmission electron micrographs of gold-doped ppCTFE with various metal volume fractions f and thicknesses t : a) $f=0.03$, $t=180$ nm; b) $f=0.11$, $t=150$ nm; c) $f=0.17$, $t=55$ nm; d) $f=0.37$, $t=50$ nm; e) $f=0.52$, $t=60$ nm.

Although various metal-polymer combinations were examined (pp C_2F_8/Co , Mo , Cu (ref. 47), co-sputtered Ekonol/Au system (refs. 23, 48), coevaporation of polyethylene/ Cu (ref. 27)) most effort has been devoted to the structural analysis of gold-containing halopolymers (refs. 4, 20, 32, 33, 47-49, 50-52). The film microstructure was studied systematically on pp C_2F_8/Au (refs. 4, 47-49) and pp CTFE/Au (refs. 50-52) composite systems. Increasing the gold volume fraction f in the layers grown on non-thermostated substrates by applying an increasing power (and U_B) to the planar magnetron covered by a gold target led to an increase of gold grain diameters from 10 nm to above 100 nm at $f = 0.52$ (Fig. 2). An important structural feature in this case is the presence of a system of smaller grains dispersed among the larger irregular particles that will play an important role during the post-annealing treatment.

The effect of the substrate temperature on the size of the metal clusters was clearly demonstrated in refs. 4, 48, 49. The change of the substrate temperature during the deposition from $-10^\circ C$ to $60^\circ C$ resulted in a substantial increase in the grain diameters. Also the post-annealing above the temperature of the main (glass-rubber) transition in the polymeric constituent at about $160^\circ C$ (refs. 4, 48, 49, 53) caused considerable increase in the grain sizes including spheroidization, coalescence and sintering of the gold clusters due to enhanced motion and migration radius of the small incorporated metal particles. The diffraction analysis (ref. 4) indicated a texturing in the (111) direction of the Au crystallites formed at room temperature. Annealing to $200^\circ C$ causes a decrease in the texturing due to a coalescence of small particles to large aggregates of twinned crystal clusters.

The composition and chemical structure of the Au/halopolymer systems was extensively studied in dependence on the preparation parameters and possible plasma surface interactions (refs. 4, 33, 48, 51). The most important result is the decrease in the halogen atom concentration when the gold volume fraction is increased as documented by AES depth profile analysis of the films (Fig. 3), infrared spectroscopy (Fig. 4) as well as by ESCA (ref. 48).

Usually, during the surface analysis (AES, ESCA etc.) the interpretation of results is to be carried out very carefully because of the actual surface modification by the applied agent (ions, electrons, photons) causing preferential sputtering, especially in the case of organic materials. Therefore, only relative changes in the film composition analysed by the same treatment are expected to yield reliable information (ref. 54).

The higher gold content in the layers is accompanied by the decrease in the halogen concentration (refs. 48, 50, 51) and the more pronounced differences between the surface and the bulk composition (refs. 33, 50, 51) (Fig. 3). The overall losses of fluorine from the layers are documented by the shift in the infrared spectra of the band due to CF_2 stretching vibrations at 1210cm^{-1} to CF stretching centered at 1100cm^{-1} (Fig. 4). These effects were explained by enhanced bombardment of the layers during the film growth. The energetic species striking the surface modify especially the polymer constituent (preferential losses of halogens), enhance the surface chemical reactivity (film surface vs. bulk differences) and indirectly support the increase in the gold grain diameters and surface roughness (refs. 50, 52).

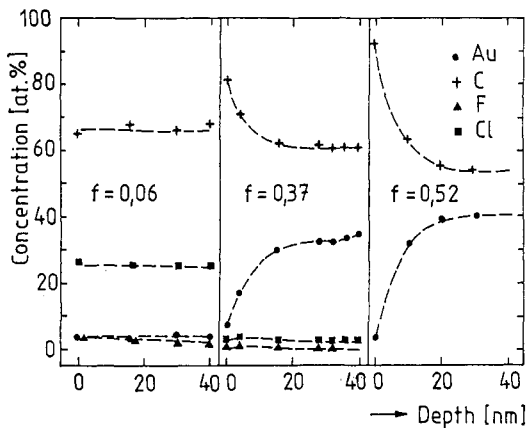


Fig. 3. AES elemental concentration depth profiles of pp CTFE films containing various gold volume fractions f .

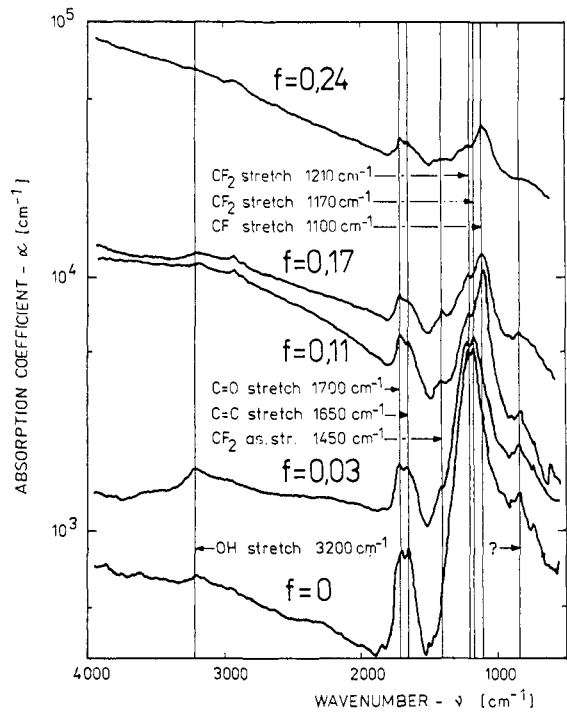


Fig. 4. IR absorption spectra of p.p. CTFE films containing various gold volume fractions.

It has been hypothesized, that the negative (predominantly gold) ions accelerated from the negatively biased powered electrode play the decisive role in this respect (refs. 23,33,50,51). The occurrence of such negative ions has been anticipated after direct measurements of the sputter-deposition of various gold-containing intermetallic compounds and a simple model for negative gold ion formation based on a difference between the ionisation potential and the electron affinity of atoms at the target surface (ref. 55). The enhanced formation of negative ions at the presence of a gold target has been confirmed by Langmuir probe measurements in our deposition system (Fig. 5) (ref. 56). The decrease of the electron saturation current after addition of CTFE to Ar clearly signifies the formation of negative ions. A preliminary analysis has disclosed that the concentration of negative ions n_- in the plasma is of the same order as the concentration of electrons. It is evidenced from Fig. 5

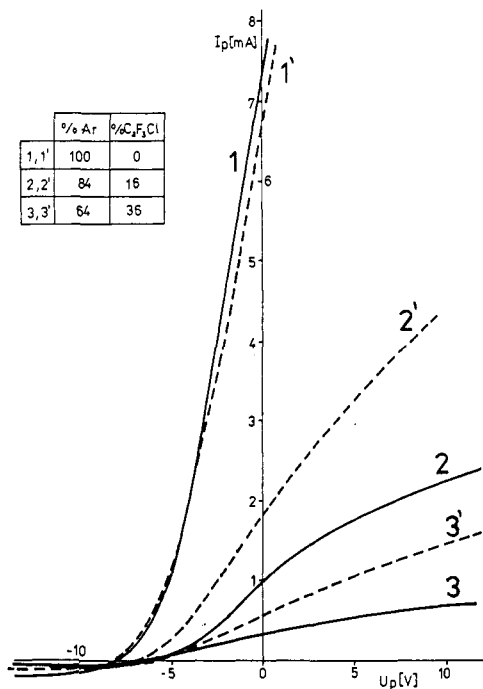


Fig. 5. Probe current I_p versus probe voltage U_p with respect to the plasma potential for various Ar/CTFE working gas mixtures and for aluminium --- and gold — targets.

that n_c is substantially higher at the presence of a gold target than in the system with an aluminium one.

Since the metal/plasma polymer films grow under nonequilibrium conditions the structural instabilities are usually inherently present and estuary in considerable aging effects at ambient atmosphere (ref. 57). In this respect the presence of incorporated free radicals and subsequent coalescence of small metal particles is important. Substantial stabilisation may be reached by vacuum post-annealing to about 80°C for 30 min in the case of ppCTFE/Au systems.

Metals/a-C:H films

Although a number of vacuum methods and sophisticated treatments for deposition of carbonaceous films have been applied, the resulting film structure is affected entirely by a single parameter - the energy flux carried by the species impacting on the growing insulating layer at the presence of a hydrocarbon gas or vapour. The plasma deposited carbon films were usually found to be amorphous (e.g. refs. 38,58,59) but partly a polycrystalline diamond structure has also been reported (e.g. refs.60,61). A model of the microstructure has been suggested (ref. 12) consisting of puckered n-fold ($n = 3-8$) rings interconnected by strong crosslinks involving tetrahedral bonds. Using an effective medium approach (ref. 37) the as-deposited films were found to contain amorphous diamond-like, amorphous graphitic and polymeric components. Upon annealing the amorphous diamond-like and polymeric components decrease, the graphitic part grows and a void component appears.

In view of further modifications of the film characteristics various metals have been incorporated into the a-C:H matrix. Cr/a-C:H and Al/a-C:H systems were prepared (refs. 8,12) in an ion plating arrangement. A decrease in the hardness when the metal fraction is increased has been observed. The diffraction data suggested that carbon atoms are incorporated between individual metal atoms of tetrahedra. After annealing above 350°C aggregation of metal crystals containing the carbides was observed. The Al/a-C:H films exhibit the Al_xC_{1-x} composition with x varying from 0.2 to 0.6. However, mechanical or thermal treatment caused fast decomposition.

Extensive work has been devoted to the investigation of metal-carbon films for solar selective absorbers (refs. 14-16). Reactive sputtering of Cu and stainless steel was performed in C_2H_2 and CH_4 gases. The metals were bonded predominantly in corresponding carbide forms.

In our laboratory Al, Cu, Ag, Ni and Au were added by evaporation into the a-C:H films grown on the excitation rf powered (negatively biased) electrode at the presence of benzene or butane (refs. 36, 10). Au, Ag and Cu were dispersed in the form of nearly spherical metal clusters (3-10 nm in diameter) in the amorphous carbon matrix. Further spherodization of the metal grains after annealing to 200°C has been observed.

When increasing the metal volume fraction the hardness of these films subsequently decreased. A typical example is shown in Fig. 6 for a Ag-doped a-C:H film grown at 40 W (-500 V bias) and 1 Pa in of the Ar (30%)/butane working gas mixture.

The stability of the structure and properties were found to be much better and the aging effects much less important than in the case of metal-containing plasma polymers.

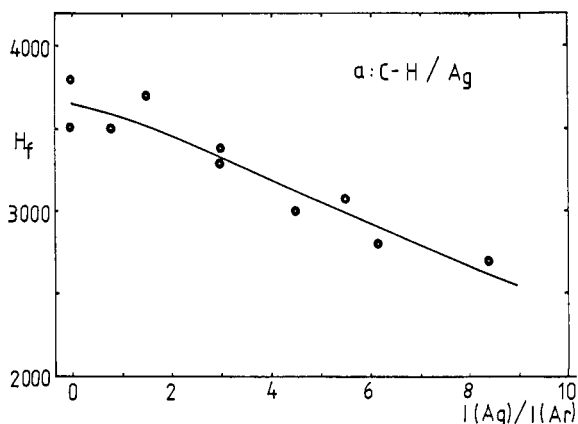


Fig. 6. The Vickers microhardness H_f (kg/mm²) as a function of increasing silver volume fraction characterized by the $I(Ag)/I(Ar)$ emission line intensity ratio.

OPTICAL PROPERTIES

Metal/plasma polymer films

In the case of metal - containing plasma polymers the anomalous optical absorption in the visible region occurs (similarly to cermets - ref. 63) that gives rise to a spectral selectivity and coloured appearance of the films. Most data have been reported on gold-doped halocarbon plasma polymers (refs. 20,32,33,47,48,50,52,64). When increasing the metal volume fraction f an absorption maximum develops near 550 nm (ref. 64). With higher f this maximum systematically shifts to longer wavelengths and the transmission at higher λ subsequently decreases. According to f various film colours may be distinguished: $f \sim 0.01$ - pink, $f \sim 0.06$ - red, $f \sim 0.24$ - violet, $f \sim 0.37$ - blue.

The optical properties with emphasis on the colour effects have been reported also for other polymer/metal combinations: HMDS/Al (ref. 21), CF_4 /Cu, Al (ref. 20), OMTS, HMDS/Ag,Au,Cu (ref.65). However, when films are prepared in a reactive gas atmosphere using a chemically active metal dopant, the tinting can be caused by the optical absorption due to the originated chemical compounds (ref.66).

After annealing the gold - halocarbon polymer films, the optical characteristics usually dramatically change (refs. 48,64). Depending on the value of f , the absorption maximum may change its form (become deeper and narrower) and position. Simultaneously, the transmission at longer wavelengths may decrease or increase according to the microstructural rearrangement responsible for these effects. Two main structural events play decisive role in this respect: losses of the polymer phase at increased temperatures and, more efficiently, the changes in the grain shape and size (spherodization, coalescence etc.). Pronounced changes were observed when the temperature was increased above its critical value that coincides with the main transition in the polymer - about 160°C in the case of pp fluorocarbon polymers (refs. 48,53). Nevertheless, also spontaneous changes in the optical characteristics during the aging of the films after the deposition have been observed (ref.57). In this case the coalescence of the metal grains is dominant as has been shown experimentally (TEM) as well as by the theoretical effective medium approach.

Effective medium (EM) approach

Independently, the EM theory has been applied to the study of gold-containing halocarbon plasma polymers in two laboratories (refs. 48,52,67). The EM approach is principally based on two assumptions (ref.68): i) The inhomogeneities are so large that each point in the material can be associated with the macroscopic dielectric function; ii) The system can be described as an EM if the random unit region, embedded in the EM, is not detectable in an experiment using electromagnetic radiation confined to a specified wavelength range. It means that the extinction of the random unit region should be the same as if it were replaced by a material with an effective dielectric function.

The condition that the inhomogeneities are substantially smaller than the wavelength of light is usually fulfilled in the case of plasma deposited composite metal-containing plasma polymers. In refs. 52,67 four models of an EM have been tested to simulate the optical behaviour of Au/ppCTFE systems: 1) the Maxwell-Garnett (MG) model (ref.69) for topologically asymmetric composites, 2) the Bruggeman self-consistent (BSC) model (ref.70) for topologically symmetric systems, 3) the "correlated three component system" (CS) (ref.71) being an extension of the BSC theory, and, finally, 4) the probabilistic growth (PG) model (ref.72) incorporating the advantages of both the MG and BSC theories.

The comparison of the experimentally obtained optical responses and theoretical predictions is illustrated in Fig. 7, when spherical grain shapes are considered. It has been shown that the PG model yields the best fit with the experiment within f up to 0.52. The PG model predicts the position and the absolute values of the maxima in n and k in the resonance region at lower f and simulates also an increasing extinction in the infrared region at higher f . On the other hand the MG model partly fits at low f (≤ 0.3) but it fails at higher f .

The optical transmission of gold-doped pp C_2F_8 films has been simulated by generalized PG and MG models for ellipsoidal particle shapes (ref.48). Agreement of the theoretical predictions based on the PG model with experimental values was obtained for as deposited as well as annealed samples. The observed broadening of the resonance peak was partially explained by considering the

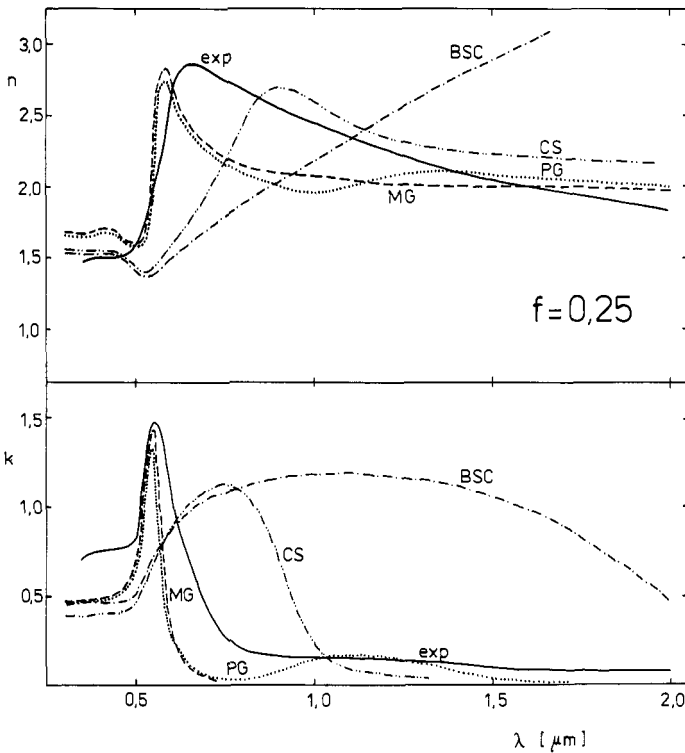


Fig. 7. Spectral dependence of optical constants n and k of a gold-doped ppCTFE film characterized by a volume fraction $f=0.25$ and the comparison with theoretical models.

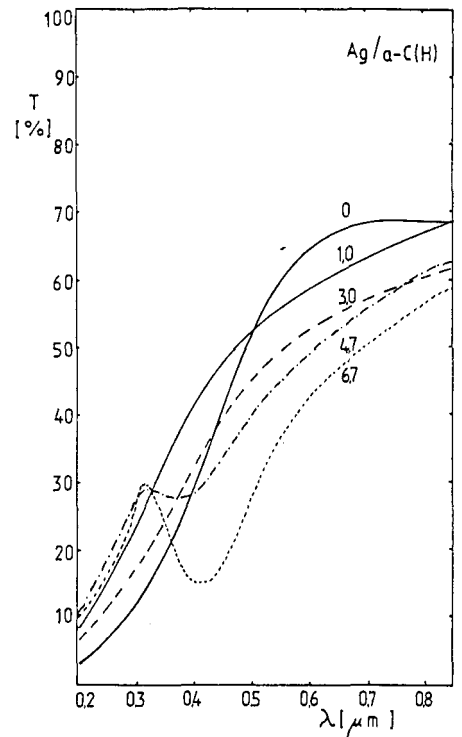


Fig. 8. Optical transmission spectra of Ag/a-C:H films. The content of Ag is indicated by the ratio of the Ag (328 nm) and the Ar (418) line intensities emitted from the discharge.

topological disorder. A three phase model based on the PG theory was proposed that could explain the possible existence of a carbon layer at the gold - PTFE interface as suggested by XPS analysis, but no distinct correspondence to the optical behaviour has been obtained.

The position of the experimental dielectric function of gold-doped ppCTFE has been studied with respect to the absolute limits (Wiener bounds) in the complex plane (ref. 52). An application of such approach for direct estimation of microstructural parameters from optical measurements has been suggested (ref.73).

Metal/a-C:H films

In contrast to plasma polymers that possess very low absorption in the visible region so that the imaginary part of the dielectric function is negligible, the carbon films exhibit higher absorption. In numerous studies the absorption coefficient - α - of a - C:H films has been measured as a function of experimental conditions-post-annealing (ref.74), CTFE concentration in the CTFE/benzene working gas mixture (ref.86) or the substrate negative bias voltage (ref.36). By plotting $(\alpha \hbar \omega)^{1/2}$ versus the photon energy $\hbar \omega$ the optical gap may be evaluated.

The effect of metal inclusions on the optical behaviour of a - C:H films has been recently studied in our laboratory. Typical transmission spectra of Ag-doped a - C:H films are shown in Fig. 8, when the Ag concentration is subsequently increased. With the growing Ag content the transmission in the near UV rises but decreases at longer wavelengths. An absorption maximum develops around 400 nm and shifts to longer λ as the amount of Ag is increased.

ELECTRICAL PROPERTIES

Composite metal/plasma polymer films

Boonthanom and White (ref. 27) measured composite copper/polyethylene films prepared by vacuum co-evaporation. The electrical characteristics of as-deposited films exhibited instabilities so in situ annealing up to 493 K was performed. This procedure converted Cu into CuO_2 islands. If the temperature of 423 K was only reached the centres of Cu remained in oxide islands. Hopping of electrons between traps in localized states close to the Fermi level was considered as a conduction mechanism.

The electrical properties of Au/pp halocarbon films were studied by Perrin et al. (ref. 49) and simultaneously in our laboratory (refs. 67,75). If one considers the dependence of dc conduction versus volume fraction, first, low value is observed as the transport processes are basically governed by electron tunneling between the gold grains. Percolation threshold is reached at a volume fraction $f_c \sim 0.4$ and conductivity phenomena become more complex. In ref. 49 in accord with usual cermet film approach the effective medium theory after Ping Sheng was shown to describe correctly the conductivity above f_c . The effect of annealing on film resistivity has been studied in the case of gold doped pp CTFE (refs. 67,75). Above 80°C the irreversible changes of the sheet resistance were observed documenting the commence of the microstructural rearrangement. The temperature dependence of the sheet resistance in the case of Au/ppCF₄ is in Fig. 9 (ref.75). The most dramatic change above percolation threshold seems to start at about 150°C . This points out the fact that polymer component approaches glass transition temperature which is likely below 200°C as indicated in ref. 53. The decrease of resistivity for samples with the volume fractions above f_c after annealing at 180°C was also observed in ref. 49. TEM observations revealed the increase of the island sizes and their coalescence especially for higher gold concentration.

As far as the ac behaviour is concerned several works on pure plasma polymers have been published (refs. 53,76,77,78). Considerable influence of oxygen and water vapour after the films are exposed to the atmosphere were reported. When metal was incorporated additional conductivity component appeared (refs. 4,77). A careful study of composite films ac behaviour and the influence of ambient atmosphere would be beneficial. Similar electrical properties of co-sputtered composite films have been found in ref. 23.

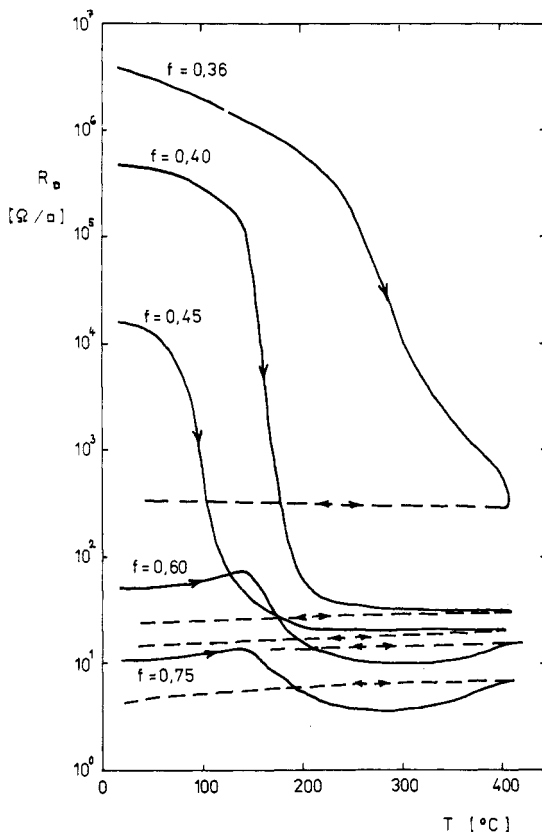


Fig. 9. The sheet resistance as a function of temperature for various gold volume fractions in pp CF₄.

Composite metal/hard carbon films

The electrical properties of plain a - C:H films have been measured by several authors (see refs. 42,79). Jones and Stewart (ref.79) have found that conductivity of their a - C:H films decreases with the monomer used in following order: methane, ethane, acetylene and ethylene and substrate temperature. Pressure in the reactor was 0.13 torr, flow rate 3-6 cm³ STP/min and $U_B = -380$ V. Phosphine, diborane and nitrogen gases have been mixed into monomer in known small amounts. The specimen conductivity increased by one and three orders of magnitude, depending on the substrate temperature. Conduction is predominantly by hopping in a region of high density of localized states for both doped and undoped samples. Doping or increased substrate temperature modified density of localized states in a way that moved the conduction path closer to the Fermi level fixed with respect to valence band. Therefore, it was suggested that doping did not take place substitutionally, as for amorphous silicon but increased the density of localized states.

In our laboratory we have studied Au and Ag/ a - C:H films. The irreversible change of resistivity occurred at temperatures between 200 and 250°C in the former case and above 250°C in the latter case. The TEM observations of these films revealed only minor changes after the annealing except that metal islands obtained more spherical shapes. It seemed that for the increased conductivity a structural change of a - C:H component of the composite was responsible. Sikkens (ref. 17) found for his co-sputtered Ni/hard carbon films that the electrical resistivity changed only a little after 2 hours annealing at 400°C. Weissmantel *et al.* (ref. 13) have also measured dc conductivity of Ti or Sn/hard carbon sputtered films as a function of metal volume. Biederman *et al.* (ref.18) found instabilities in the electrical properties of Ag/hard carbon sputtered films caused by aging effects.

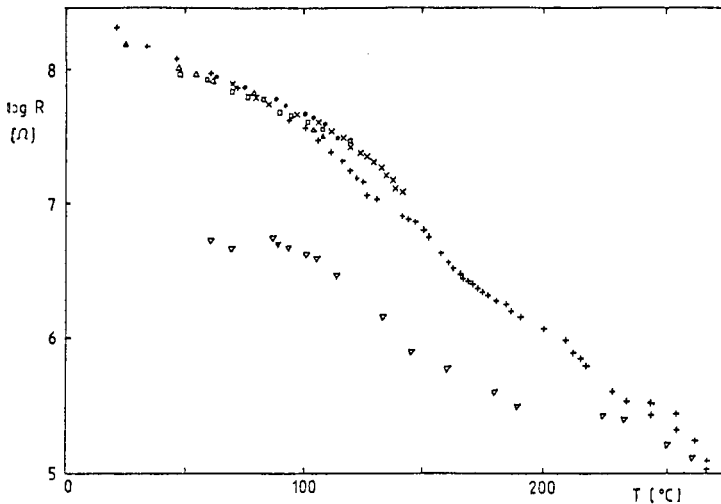


Fig. 10. The resistance R of a gold-containing a - C:H film versus temperature T (working gas mixture: Ar/butane, 3 Pa, $U_B = -500$ V, 40 W rf power). The subsequent annealing cycles: temperature increase: $\bullet \Delta \square \times +$ and decrease: ∇ .

CONCLUSIONS

Deposition processes and basic physical properties of both-composite metal plasma polymer and metal/hard carbon films have been briefly reviewed from the present state of knowledge. Several applications have been proposed. Let us mention few examples. In optics the discussed films were suggested as large area optical filters or decorative coatings (ref. 21) and for optical recording (refs. 80,81). In microelectronics (VLSI technology) Morita and Hattori described dry lithography involving an X-ray mask from gold doped poly styrene (ref. 82). Metal/hard carbon films were suggested for improvement of electrical contacts (ref. 13). However, there are still several problems in the production of the discussed films and their post-deposition behaviour which have to be fully understood before wider application will be possible.

REFERENCES

1. B. Abeles, Appl. Solid State Sci., **6**, 1 (1976).
2. E. Kay and A. Dilks, J. Vac.Sci.Technol., **18**(1), 1(1981).
3. H. Biederman, Proc. Vacuum '86 Conference, Glasgow, March 1986, to be published in Vacuum.
4. E. Kay, Z.Phys. D - Atoms, Molecules and Clusters, **3**(251)(1986).
5. H. Biederman, Thin Solid Films, **86**,125(1981).
6. L. Holland, L. Laurenson, R.E. Hurley and K. Williams, Nucl.Instrum.Meth., **111**,555(1973).
7. L. Holland, British Patent Application, **1**, 582,231(1976).
8. Ch. Weissmantel, Proc. IX. Int.Vac.Congr./V Int. Conf.Surf.Sci.,Madrid 1983, p.299.
9. H. Biederman and I. Chudáček, to be published in J.Appl.Polym.Sci.
10. H. Biederman, I. Chudáček, D. Slavínská, L. Martinů, J. David, S.Nešpůrek, Proc. 5th Int.Conf.Polymer Physics,High Tatres,Czechoslovakia, April 21-25,1987,p.110, to be published in Vacuum.
11. H. Biederman, R.P.Howson, ibid.
12. Ch. Weissmantel, K. Brener and B. Winde, Thin Solid Films,**100**,383(1983).
13. Ch. Weissmantel, E. Ackerman, K. Bewilogua, G. Hecht, H. Kupfer and B.Rau, J.Vac.Sci.Technol.A,**4**(6),2892(1986).
14. G.L.Harding and S. Craig, J.Vac.Sci.Technol.,**16**(3),857(1979).
15. S.Craig and G.L.Harding, Thin Solid Films, **97**,345(1982).
16. S.Craig and G.L.Harding, Thin Solid Films,**101**, 97(1983).
17. M.Sikkens, Solar Energy Mater.,**6**, 403(1982).
18. H. Biederman, R.P.Howson and I. Mc Cabe, Proc.IPAT 1987,Brighton (UK).
19. E.Kay, A.Dilks,V.Hetzler, Macromol.Sci.:Chem. A, **12**, 1393(1978).
20. H. Biederman and L. Holland, Nucl. Instrum.Methods,**219**,497(1983).
21. R.F.Wielonski and H.A.Beale, Thin Solid Films,**84**,425(1981).
22. Y. Asano, Thin Solid Films,**105**,1(1983).
23. R.A. Roy, R. Messier and S.V. Krishnaswamy, Thin Solid Films,**109**,27(1983).
24. B.V. Tkaszuk, V.M.Kolotyarkin: Poluczenije tonkich polimernychplenok iz gazovoj fazy. Chimija Moskva 1977.
25. E. Kny, L.L. Levenson, W.J. James and R.A. Auerbach, J.Phys.Chem.**84**,1635 (1980).
26. N.Inagaki, T.Nishio, K. Katsuura, J.Polymer Sci.: Polymer Lett. Ed.,**18**, 765(1980).
27. N.Boonthanom and M. White, Thin Solid Films,**24**,395(1974).
28. J.L.Vossen, in: Thin Film Processes (J.L.Vossen and W.Kern eds.),Academic Press, New York 1978.
29. H. Yasuda, ibid.
30. M. Shen and A.T.Bell, ACS Symp. Ser.108, (M.Shen and A.T.Bell eds.), Washington DC(1979),p.1.
31. R. d'Agostino, P. Capezzuto, G. Bruno and F. Cramarossa, Pure Appl.Chem. **57**(9),1287(1985).
32. H. Biederman, Vacuum, **34**, 405(1984).
33. L. Martinů, H. Biederman and J. Zemek, Vacuum,**35**,171(1985).
34. J. Janča, M. Drštička and R.Čevelík, Scripta Fac.Sci.Nat.Univ.Purk.Brun., **15**(5),251(1985).
35. H. Biederman, L. Martinů, unpublished results.
36. H. Biederman, L. Martinů and J. Zemek, Vacuum,**35**, 447(1985).
37. F.W. Smith, J.Appl.Phys.,**55**, 764 (1984).
38. A.R.Nyaiesh and L. Holland, Vacuum, **34**, 519(1984).
39. B. Dischler, A. Butenzer and P. Koidl, Solid State Commun.,**48**, 105(1983).
40. R.E.Sah, B. Dischler, A. Bubenzer, P. Koidl, Appl.Phys.Lett.,**46**, 739 (1985).
41. R.Memming, Thin Solid Films, **143**, 279(1986).
42. J.C. Angus, P. Koidl and S. Domitz, in: Plasma Deposition of Thin Films (J.Mort, F.Jansen eds.), CRC Press,1986.
43. J.A. Woolham, Hao Chang and V. Natarajan, Appl.Phys.Commun.,**5**(4), 263 (1985-6).
44. B. Window and N. Savvides, J.Vac.Sci.Technol.A, **4**(3),453(1986).
45. L. Martinů, H. Biederman, Plasma Chemistry and Plasma Processing,**5**,81 (1985).
46. P. Špatenka, PhD thesis, Charles University, Prague 1986.
47. E. Kay and M. Hecq, J.Appl.Phys.,**55**, 370(1984).
48. J. Perrin, B. Despax and E. Kay, Phys.Rev.B,**32**, 719(1985).
49. J. Perrin, V. Hanchett, B. Despax, E. Kay, J.Vac.Sci.Technol.A,**4**(1),46 (1986).
50. L. Martinů and H. Biederman, J.Vac.Sci.TechnolA,**3**(6)(1985) 2639.
51. L. Martinů, Thin Solid Films,**140**,307(1986).
52. L. Martinů, Solar Energy Mater.,**15**, 21(1987).

53. L. Martinů, H. Biederman and J. Nedbal, Thin Solid Films, **136**, 11(1986).
54. L. Eckertová and L. Martinů, Proc. 6th Int.Symp. on Elementary Processes and Chemical Reactions in Low Temp.Plasmas, Jelšava(Czechoslovakia)June 9-13,1986,p.41.
55. J.J. Cuomo, R.J. Gambino, J.M.E. Harper and J.D. Kuptsis, IBM J.Res.Dev. **21**, 580(1977).
56. L. Martinů, P. Špatenka, H. Biederman and M. Šícha, Thin Solid Films,**141**, L83(1986).
57. H. Biederman, L. Martinů and S. Nešpůrek, to be published.
58. T.J. Moravec, T.W. Orent, J.Vac.Sci.Technol.,**18**,226(1981).
59. A. Bubbenzer, B. Dischler, G. Brand and P. Koidl, J.Appl.Phys.,**54**,4590 (1983).
60. S. Berg, L.P. Anderson, Thin Solid Films,**58**,117(1979).
61. T. Mori, Y. Namba, J. Vac. Sci. Technol. A, **1**, 23(1983).
62. Ch. Weissmantel, K. Bewilogua, D. Deitrich, U. Ebersbach, H.J. Erler, B. Rau and G. Reisse, Thin Solid Films, **96**, 31 (1982).
63. Yu. I. Petrov, Fizika Malych Častic, Nauka, Moskva 1982 (in Russian) and ref.therein.
64. L. Martinů and H. Biederman, Vacuum, **36**, 477(1986).
65. J. Janča, P. Pavelka, Scripta Fac.Sci.Nat.Univ.Purk.Brun.,**15**(5)261(1985) Phys.
66. M. Hecq, P. Ziemann, E. Kay, J. Vac. Sci.Technol.A, **1**(2),364(1983).
67. L. Martinů, PhD thesis, Charles University, Prague, January 1985.
68. G.A. Niklasson, C.G.Granqvist and O. Hunderi, Appl.Opt.**20**,26(1981).
69. J.C. Maxwell - Garnett, Philos.Trans.R.Soc.London,**203**, 385(1904) and **205**, 237 (1906).
70. D.A.G. Bruggeman, Ann.Phys.Leipzig,**24**,636(1935).
71. D.M. Wood and N.W.Ashcroft, Philos.Mag.,**35**, 269(1977).
72. Ping Sheng, Phys.Rev.Lett.,**45**, 60(1980).
73. L. Martinů and A. Fejfar, Materials Sci., in the press.
74. D. A. Anderson, Philos.Mag.,**35**, 17(1977).
75. L. Martinů, Solar Energy Mater., **15**, 135(1987).
76. H. Biederman, Vacuum, **31**, 285(1981).
77. H. Biederman and P. Meek, unpublished results.
78. U. Helzler, E. Kay, J.Appl.Phys., **49**, 5617(1978).
79. D.I. Jones and A.D. Stewart, Philos.Mag.,**46**, 423(1982).
80. H. Yamazaki and Y. Asano, Jpn. J. Appl.Phys.,**21**, L 673(1982).
81. Y. Takeoka and N. Yasuda, Proc. ISIAT '83 and IPAT '83, Kyoto 1983,p.993.
82. S. Morita and S. Hattori, Pure Appl. Chem.,**57**, 1277(1985).